Journal of Anatomy

J. Anat. (2015) **226**, pp478–488 doi: 10.1111/joa.12296

Accumulation of type VI collagen in the primary osteon of the rat femur during postnatal development

Yukihiro Kohara,[1] Satoshi Soeta,[1] Yayoi Izu[2] and Hajime Amasaki[1]

[1]*Laboratory of Veterinary Anatomy, Nippon Veterinary and Life Science University, Tokyo, Japan*
[2]*Department of Molecular Pharmacology, Medical Research Institute, Tokyo Medical and Dental University, Tokyo, Japan*

Abstract

In rodents, the long bone diaphysis is expanded by forming primary osteons at the periosteal surface of the cortical bone. This ossification process is thought to be regulated by the microenvironment in the periosteum. Type VI collagen (Col VI), a component of the extracellular matrix (ECM) in the periosteum, is involved in osteoblast differentiation at early stages. In several cell types, Col VI interacts with NG2 on the cytoplasmic membrane to promote cell proliferation, spreading and motility. However, the detailed functions of Col VI and NG2 in the ossification process in the periosteum are still under investigation. In this study, to clarify the relationship between localization of Col VI and formation of the primary osteon, we examined the distribution of Col VI and osteoblast lineages expressing NG2 in the periosteum of rat femoral diaphysis during postnatal growing periods by immunohistochemistry. Primary osteons enclosing the osteonal cavity were clearly identified in the cortical bone from 2 weeks old. The size of the osteonal cavities decreased from the outer to the inner region of the cortical bone. In addition, the osteonal cavities of newly formed primary osteons at the outermost region started to decrease in size after rats reached the age of 4 weeks. Immunohistochemistry revealed concentrated localization of Col VI in the ECM in the osteonal cavity. Col VI-immunoreactive areas were reduced and they disappeared as the osteonal cavities became smaller from the outer to the inner region. In the osteonal cavities of the outer cortical regions, Runx2-immunoreactive spindle-shaped cells and mature osteoblasts were detected in Col VI-immunoreactive areas. The numbers of Runx2-immunoreactive cells were significantly higher in the osteonal cavities than in the osteogenic layers from 2 to 4 weeks. Most of these Runx2-immunoreactive cells showed NG2-immunoreactivity. Furthermore, PCNA-immunoreactivity was detected in the Runx2-immunoreactive spindle cells in the osteonal cavities. These results indicate that Col VI provides a characteristic microenvironment in the osteonal cavity of the primary osteon, and that differentiation and proliferation of the osteoblast lineage occur in the Col VI-immunoreactive area. Interaction of Col VI and NG2 may be involved in the structural organization of the primary osteon by regulating osteoblast lineages.

Key words: intramembranous ossification; NG2; osteoblast; primary osteon; type VI collagen.

Introduction

In rats, cortical bones of the long bone diaphysis are constructed with primary osteons via intramembranous ossification during growth periods; these bones are termed primary osteonal bones. With maturation, the primary osteons are gradually replaced by secondary osteons (Enlow & Brown, 1958; Stover et al. 1992). The primary osteon possesses a cylindrical structure arranged along the long axis of the long bone, enclosing soft tissue space with the blood vessels in the center (osteonal cavity). Although it is widely known that the secondary osteons have resorption lines, which provide proof of osteoclast resorption, the primary osteon does not have a resorption line. New primary osteons arise from the surface of the cortical bone and envelop blood vessels in the periosteum to form the osteonal cavity (Enlow & Brown, 1958; Stover et al. 1992), which suggests a relationship between primary osteon formation and vessel localization. Indeed, it has been reported that vascular endothelial cells and/or perivascular cells have an important role in osteoblast development and function (Satomi-Kobayashi et al. 2012; Weyand & von Schroeder, 2013; Ramasamy et al. 2014). Therefore, it is possible that the perivascular microenvironment regulates the formation of the primary osteon in the periosteum.

The periosteum is a specialized connective tissue comprised of two layers: the outer fibrous layer, consisting

Correspondence
Satoshi Soeta, Laboratory of Veterinary Anatomy, Nippon Veterinary and Life Science University, 1-7-1 Kyonan-cho, Musashino-shi, Tokyo 180-8602, Japan. E: s-soeta@nvlu.ac.jp

Accepted for publication *13 February 2015*
Article published online *5 May 2015*

mainly of fibroblasts and elastic fibers; and the inner osteogenic layer, consisting of mesenchymal stromal cells and osteoblast lineage cells (Tonna, 1974; Mulliken & Glowacki, 1980; Ham, 1987; Fan et al. 2008). Fan et al. (2008) suggested that osteoprogenitor cells differentiated into mature osteoblasts in the osteogenic layer. The periosteum contains many types of extracellular matrix (ECM), such as type I, III, IV and VI collagens, laminin, tenascin and fibronectin (Carter et al. 1991; Everts et al. 1998; Nilsson et al. 1998). The ECM not only provides a scaffold for cells, but also regulates cell migration, proliferation, differentiation and maturation by its specific cell-surface receptors (Izu et al. 2010; Mathews et al. 2012; Gattazzo et al. 2014). Therefore, in the process of osteoblast differentiation, cell adhesion to a specific ECM is thought to be crucial for the differentiation and maturation of osteoblast lineage cells in the periosteum.

Type VI collagen (Col VI) is an ECM component distributed in many connective tissues, including tendons, ligaments, muscles, skin, cornea, cartilage, bone tissue and periosteum (Everts et al. 1998). A characterized form of Col VI is a heterotrimeric protein consisting of three different α-chains: α1 (VI), α2(VI) and α3(VI); or α4(VI), α5(VI) and α6(VI) instead of α3(VI) (Fitzgerald et al. 2008; Gara et al. 2008). Col VI interacts with a large number of ECM components (i.e. type I, II, IV and XIV collagens, microfibril-associated glycoprotein-1, perlecan, decorin, biglycan, hyaluronan, heparin and fibronectin), and is proposed to integrate these molecules. In addition, previous studies revealed that Col VI is involved in various cellular interactions, such as cell adhesion (Bashey et al. 1993), migration (Burg et al. 1996) and apoptosis (Rühl et al. 1999b) via binding to cell-surface molecules, including the integrins α1β1, α2β1, α3β1, α5β1 and α10β1 (Wayner & Carter, 1987; Doane et al. 1992; Pfaff et al. 1993; Tulla et al. 2001; Hu et al. 2002) and the chondroitin sulfate proteoglycan NG2 (Stallcup et al. 1990; Nishiyama & Stallcup, 1993; Burg et al. 1996; Tillet et al. 1997, 2002). In bone tissues, Col VI has been suggested to play an important role in normal bone formation. *Col6a1*-deficient mice displayed a reduction in bone mineral density and cancellous bone mass (Christensen et al. 2012; Izu et al. 2012). In addition, Col VI deficiency altered the osteoblast arrangement in bone-forming sites. Several *in vitro* studies indicated that osteoblast-lineage cells required attachment to Col VI at early stages of differentiation (Ishibashi et al. 1999; Harumiya et al. 2002). Therefore, Col VI may regulate osteoblast behavior in bone-forming sites.

Recently, Fukushi et al. (2003) demonstrated that NG2 expression was transiently upregulated in osteoblasts in the periosteum and the cancellous bone during development of long bones. In non-osteogenic cells, NG2 promotes cell spreading and motility in response to Col VI, indicating that the interaction of NG2 with Col VI triggers transmembrane signaling events that lead to dynamic rearrangements of the actin cytoskeleton. Thus, it is possible that NG2 serves as a cell-surface receptor that regulates osteoblast lineages by binding to Col VI in the periosteum. However, the detailed functions of Col VI and NG2 in the process of the membranous ossification in the periosteum have not been elucidated.

In the present study, we demonstrate the localization of Col VI and NG2 in association with the formation of the primary osteon and osteoblast differentiation in the periosteum of the femoral diaphysis of rats during postnatal development.

Materials and methods

Animals

The animal protocols used in this study were approved by the Nippon Veterinary and Life Science University Institutional Animal Care and Use Committee. In this study, 30 male Wistar rats aged 1 day, 1, 2, 3, 4, 5, 6 and 7 weeks, and 2 and 3 months (three rats each) were used. The animals were maintained in the Life Science Research Center, Nippon Veterinary and Life Science University. Under deep anesthesia with pentobarbital (50 mg kg^{-1}, i.p.), the rats were perfused through the left ventricle with saline, followed by 4% paraformaldehyde in 0.1 M phosphate buffer (PB; pH 7.4). Femurs were immediately removed and immersed in the same fixatives for an additional 24 h at 4 °C. The specimens were decalcified with 10% EDTA-2Na in 0.01 M PB, cut into transverse slices in the femur mid-diaphysis and embedded in paraffin, according to the standard procedure. Three-micrometer-thick sections were cut and stained with hematoxylin and eosin (HE), or processed for lectin histochemistry and immunohistochemistry.

Lectin-histochemistry for griffonia simplicifolia lectin (GSL)-I

Lectin-histochemistry was performed according to Soeta et al. (2000). Briefly, after blocking of endogenous peroxidase activity, sections were treated with 1% bovine serum albumin in 0.01 M phosphate-buffered saline (PBS; pH 7.4). The sections were then incubated overnight with biotinylated GSL-I (1 : 2500; Vector Labs, Burlingame, CA, USA) at 4 °C. After the sections were overlaid with streptavidin-biotin-peroxidase complex (sABC, DAKO, Glostrup, Denmark), the reaction product was visualized with DAB solution (EnVision+, DAKO). Finally, the sections were counterstained with hematoxylin.

Immunohistochemistry

Primary antibodies used in this study are shown in Table 1. After the blocking of endogenous peroxidase activity, the sections were treated with 10 mg mL^{-1} hyaluronidase (SIGMA, Tokyo, Japan)/0.025% Triton X-100 in 0.01 M PBS at 37 °C for 30 min (for Col VI), or incubated in 0.01 M citrate buffer (pH 6.0) at 60 °C for 60 min (for Runx2, NG2 and PCNA). After the treatment with 10% normal goat serum (DAKO) in PBS (for Col VI) or Block Ace (Snow Brand Milk Products, Tokyo, Japan; for Runx2, NG2 and PCNA), the sections were incubated with anti-Col VI, anti-Runx2, anti-NG2 or anti-PCNA antibody. After washing in PBS, the sections were

Table 1 Primary antibodies used in this study.

Antibodies	Host species	Dilution (fluorescence)	Supplier	Article no.
Col VI	Rabbit	1 : 150,000 (1 : 10,000)	LSL (Tokyo, Japan)	LB-1697
Runx2	Goat	1 : 200 (1 : 200)	Santa Cruz Biotech. (Santa Cruz, CA)	sc-12488
PCNA	Mouse	1 : 5,000 (1 : 5,000)	Dako (Glostrup, Denmark)	M0879
NG2	Rabbit	1 : 100 (1 : 20)	Chemicon (Temecula, CA)	AB5320

incubated with horseradish peroxidase-conjugated antibodies against rabbit Ig (EnVision™, DAKO; for Col VI and NG2), mouse Ig (EnVision™, DAKO; for PCNA) or goat Ig (Histofine Simple Stain MAX-PO, Nichirei, Tokyo, Japan; for Runx2). Development of the reaction products and counterstaining were performed as described above.

Double-labeling immunohistochemistry

The following combinations of antibodies were used for double-labeling immunohistochemistry: anti-Col VI and anti-Runx2; anti-NG2 and anti-Runx2; and anti-PCNA and anti-Runx2. The antigen–antibody reactivities were detected with a mix of Alexa Fluor 488-conjugated anti-rabbit IgG chicken antibody (1 : 400; Invitrogen, Carlsbad, CA, USA) and Alexa Fluor 594-conjugated anti-goat IgG donkey antibody (1 : 400; Invitrogen), or Alexa Fluor 488-conjugated anti-mouse IgG donkey antibody (1 : 400; Invitrogen) and Alexa Fluor 594-conjugated anti-goat IgG donkey antibody (1 : 400; Invitrogen).

Double-labeling immunohistochemistry with anti-NG2 and anti-Col VI antibodies (both raised in rabbit) was performed according to the protocol outlined by Jackson ImmunoResearch Laboratories. After the sections were incubated with anti-NG2, the immunoreactivity was detected with an excess amount of Alexa Fluor 488-conjugate anti-rabbit IgG donkey Fab fragment (H+L; 1 : 60; Jackson ImmunoResearch, West Grove, PA, USA). After washing in PBS, the sections were incubated with anti-Col VI antibody, followed by treatment with Alexa Fluor 594-conjugated anti-rabbit IgG goat antibody (1 : 400; Invitrogen). The sections were examined with DP2-BSW software (Olympus, Tokyo, Japan).

Quantitative evaluation of primary osteon and Col VI-immunoreactive areas

To evaluate age-dependent changes of the osteonal cavity area and Col VI-immunoreactive area in the osteonal cavity of the newly formed primary osteons, 10 primary osteons were randomly selected at the outermost region of the cortical bone in three transverse sections from each animal. The osteonal cavity areas and Col VI-immunoreactive areas in the osteonal cavities were measured using IMAGEJ software (National Institutes of Health) and described as the mean of 10 primary osteons. The percentage of Col VI-immunoreactive area to the osteonal cavity area was calculated and expressed as the mean of 10 primary osteons.

To analyze the relationship between maturation of the primary osteon and the Col VI-immunoreactive area in the osteonal cavity, transverse sections of the femur obtained from three rats at 7 weeks old were used. In each section, 10 radial zones of 0.2 mm width from the periosteal to the endosteal regions were randomly selected. The thickness of each radial zone was divided into three concentric layers from the periosteal to the endosteal regions, and then the osteonal cavity area and Col VI-immunoreactive area were measured in each layer. The values were described as the means of the areas per primary osteon in each layer in three sections from each animal.

Statistical analyses were performed with one-way ANOVA and Tukey *post hoc* test.

Calculation of Runx2 and PCNA labeling index

To determine the number of osteoblast lineages (Runx2-positive) and proliferating cells (PCNA-positive) in the periosteum, immunoreactive cells were counted in the primary osteon and the osteogenic layer in three sections obtained from each animal. Runx2 and PCNA labeling index were determined by dividing the number of immunoreactive cells by the total number of cells counted ($n = 100$) in the primary osteons or the osteogenic layer, and were expressed as the mean percentage of three sections.

Statistical analyses were performed with Student's *t*-test or one-way ANOVA and Tukey *post hoc* test.

Results

Histology

At 1 day and 1 week old, the cortical bone of the femoral diaphysis showed cancellous structures with expanded vascular cavities and thin bone trabeculae. These vascular cavities often extended to the periosteum and endosteal bone marrow cavity. No clear primary osteon was detected in the cortical bone. In the osteogenic layer of the periosteum of 1-week-old rats, many spindle cells were detected in the upper region, whereas cuboid-shaped osteoblasts lined the periosteal surface of the cortical bone (Fig. 1A).

At 2 and 3 weeks old, the cortical bone showed a plexiform structure and contained many primary osteons enclosing osteonal cavities with blood vessels in their center (complete primary osteons). At the periosteal surface of the cortical bone, most of the primary osteons incompletely enclosed osteonal cavities (incomplete primary osteons), showing a pocket-like structure between two ridges of bone trabeculae in the transverse sections (Fig. 1B). In the osteonal cavities of the incomplete and complete primary osteon, spindle-shaped cells were distributed in the perivascular area and cuboid-shaped osteoblasts were arranged on the bone tissue surrounding the osteonal cavity (Fig. 1C). As shown in 1-week-old rats, the osteogenic layer of the

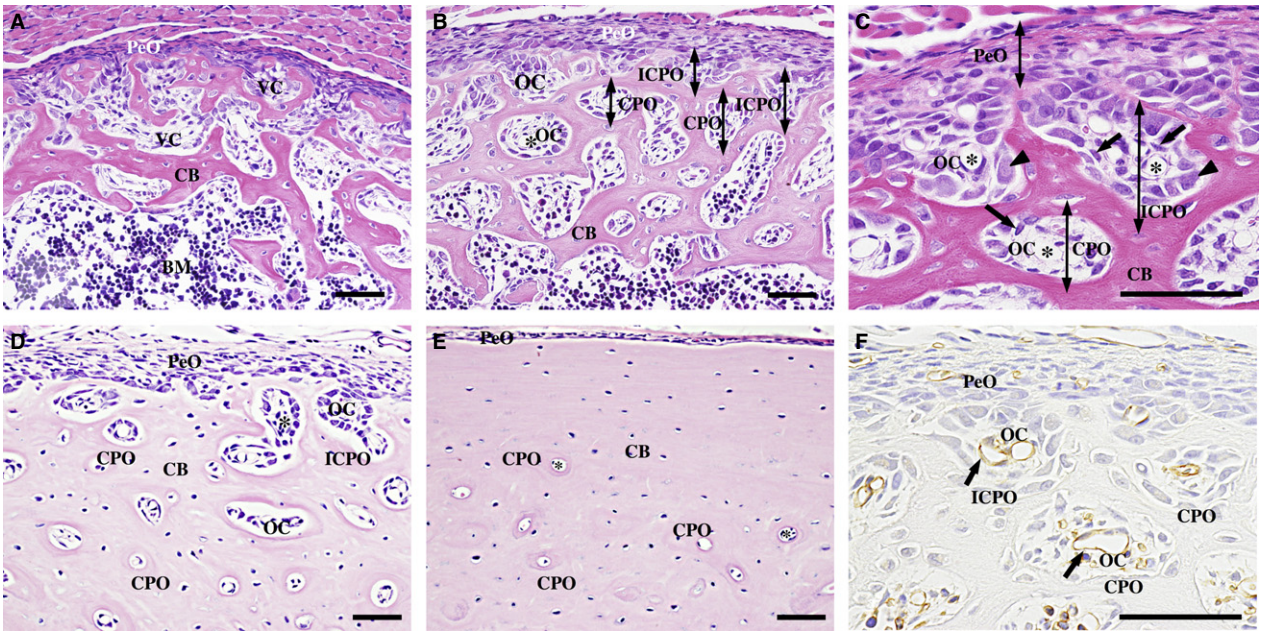

Fig. 1 Histology of the femoral diaphysis. (A) At 1 day old, the cortical bone (CB) shows a cancellous structure without clear primary osteons. (B) At 2 weeks old, the CB contains many incomplete (ICPO) and complete primary osteons (CPO) with a round osteonal cavity (OC). (C) In the OCs, spindle cells (arrows) localize in the perivascular areas, and cuboidal osteoblasts (arrowheads) line the surface of the CB. (D) At 7 weeks old, the CB shows a compact structure and the OCs are decreased from the outer toward the inner cortical region. (E) At 3 months old, no ICPOs are detected. (F) GSL-I-reactive blood vessels (arrows) are observed in the center of the CPOs and ICPOs. PeO, periosteum; VC, vascular cavity; BM, bone marrow; asterisk, blood vessel. Scale bars: 50 μm. (A–E) HE staining. (F) GSL-I lectin-histochemistry.

periosteum consisted of spindle cells in the upper region and cuboid-shaped osteoblasts on the periosteal surface of the cortical bone.

From 4 to 7 weeks old, the cortical bone became more compact and the osteonal cavity area was significantly decreased from the outer towards the inner cortical region (outer vs. middle; $P < 0.001$; outer vs. inner; $P < 0.001$; Fig. 3B). The incomplete primary osteons also decreased in number or disappeared, especially in the cranial region of the diaphysis (Fig. 1D).

At 2 and 3 months, incomplete primary osteons were not detected, and the periosteal surface of the cortical bone was smooth. The osteonal cavities of the primary osteons in the outer cortical regions decreased in size with age (3 months vs. 2 weeks; $P < 0.001$; vs. 4 weeks; $P < 0.001$; vs. 7 weeks; $P < 0.01$; Fig. 3C). Most of the primary osteons contained a few osteoblasts lining the perivascular surface of the bone tissue. In the periosteum, the osteogenic layer became thinner and consisted of a few layers of small osteoblasts (Fig. 1E).

GSL-I lectin-histochemistry

As Alroy et al. (1987) previously described, GSL-I reactivity was found in the endothelial cells of the blood vessels. GSL-I histochemistry clearly demonstrated the presence of blood vessels in the osteonal cavities of the incomplete and complete primary osteons (Fig. 1F).

Col VI -immunohistochemistry

At 1 day and 1 week old, Col VI-immunohistochemistry showed a faint fibrous immunoreactivity in the ECM in the vascular cavity of the cortical bone (Fig. 2A).

From 2 to 7 weeks old, Col VI-immunoreactivity became more intense in the ECM in the osteonal cavities of the incomplete and complete primary osteons (Fig. 2B–D). At 7 weeks old, the Col VI-immunoreactive area was significantly decreased, as the osteonal cavity became smaller from the outer toward the inner cortical regions (outer vs. middle; $P < 0.001$; outer vs. inner; $P < 0.001$; middle vs. inner; $P < 0.01$; Fig. 3B).

At 2 and 3 months old, Col VI-immunoreactivity was not observed in the femoral diaphysis (Fig. 2E). The Col VI-immunoreactive area of the osteonal cavity in the outermost cortical region was significantly lower at an age of 3 months compared with 2 and 4 weeks ($P < 0.05$ and $P < 0.001$, respectively; Fig. 3C). The percentage of the Col VI-immunoreactive area to the osteonal cavity area was also significantly decreased compared with that at 2, 4 and 7 weeks old ($P < 0.05$, $P < 0.01$ and $P < 0.001$, respectively; Fig. 3C).

Runx2-immunohistochemistry

At 1 day and 1 week old, Runx2-immunoreactivity was identified in nuclei and the cytoplasm of osteoblasts lining the

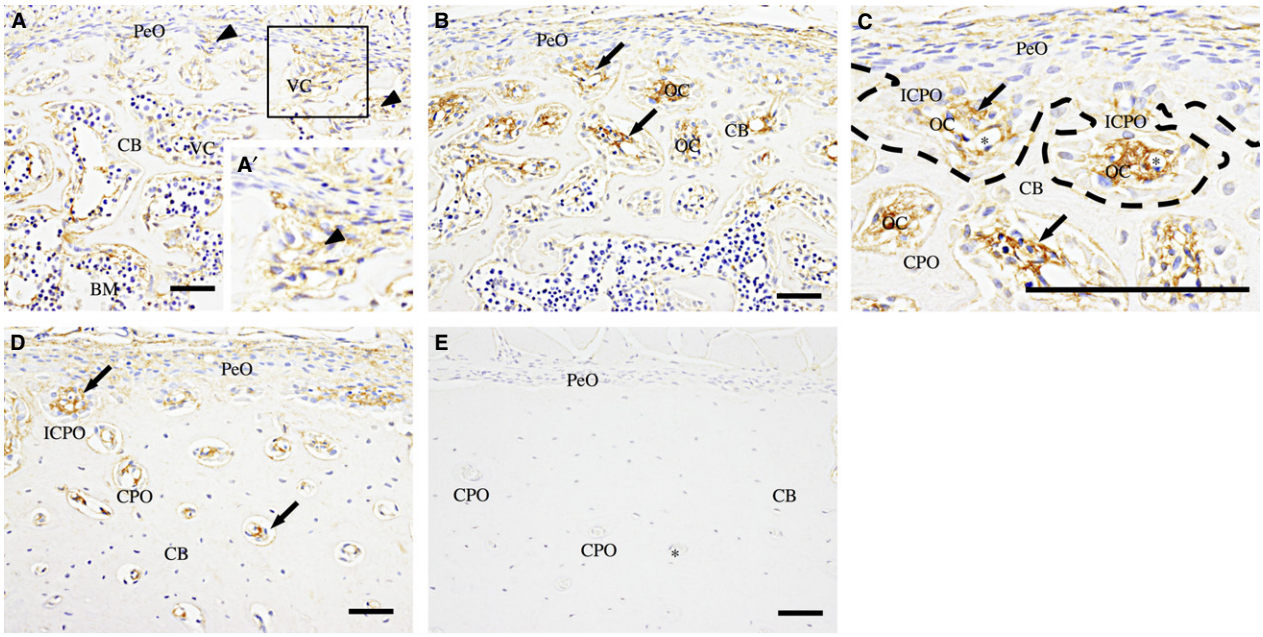

Fig. 2 Col VI-immunohistochemistry of the femoral diaphysis. (A) At 1 day old, faint fibrous immunoreactivity (arrowheads) is detected in the ECM in the vascular cavity (VC) of the cortical bone (CB). (A′) A high-magnification view of the boxed area. (B) At 2 weeks, the immunoreactivity (arrows) is more intense in the ECM in the osteonal cavities (OC) of incomplete (ICPO) and complete primary osteons (CPO). (C) A high-magnification view of the periosteal cortical region of (B). In the ICPOs, bone trabeculae (dotted line) extend to enclose the immunoreactive areas (arrows). (D) At 7 weeks old, immunoreactive ECM (arrows) is decreased in the CPOs as the OCs become smaller from the outer region toward the endosteal region. (E) At 3 months old, no immunoreactivity is observed. PeO, periosteum; BM, bone marrow; asterisk, blood vessel. Scale bars: 50 μm.

bone surface and in some spindle cells in the vascular cavities. The nuclear immunoreactivity was more intense than the cytoplasmic immunoreactivity. However, immunoreactive cells were sparingly detected in the periosteum (data not shown).

From 2 to 6 weeks old, many Runx2-immunoreactive cells were detected in the osteonal cavity of the incomplete and complete primary osteons in the outer cortical region. These cells consisted of cuboid-shaped osteoblasts lining the perivascular bone surface and small spindle cells in the perivascular area. In the periosteum, the immunoreactivity was detected in a small number of the spindle cells (Fig. 4A).

At 7 weeks old, Runx2-immunoreactive cells were detected in the incomplete and complete primary osteons in the uppermost region of the cortical bone, but not in the complete primary osteons in the inner region of the cortical bone (Fig. 4B).

At 2 and 3 months old, Runx2-immunoreactive cells were sparingly detected in the osteonal cavity of the primary osteon and in the periosteum (Fig. 4C).

The Runx2 labeling index was significantly higher in the osteonal cavity than in the osteogenic layer at 2 weeks, 4 weeks and 3 months old ($P < 0.05$, $P < 0.05$ and $P < 0.05$, respectively; Fig. 4G). In addition, its value in the osteonal cavity of the outer cortical region started to decrease at 4 weeks old, and was significantly lower at 3 months than at 4 weeks ($P < 0.05$; Fig. 4G).

Double-immunofluorescence staining for Runx2 and Col VI clearly demonstrated the localization of Runx2-immunoreactive spindle cells and osteoblasts in the Col VI-immunoreactive ECM in the incomplete and complete primary osteons at 2 weeks old (Fig. 4D–F).

PCNA-immunohistochemistry

At 1 day and 1 week of age, PCNA-immunoreactivity was detected in the nuclei of many spindle-shaped cells in the osteogenic layer of the periosteum and in the vascular cavity of the cortical bone (data not shown).

From 2 to 7 weeks old, many PCNA-immunoreactive cells were detected in the osteonal cavity of the incomplete and complete primary osteons in the outer region of the cortical bone (Fig. 5A,B). However, in the periosteum, immunoreactivity was detected in a small number of spindle cells. The PCNA labeling index was significantly higher in the primary osteons than in the osteogenic layers at 2, 4 and 7 weeks old ($P < 0.05$, $P < 0.01$ and $P < 0.01$, respectively; Fig. 5G).

At 2 and 3 months old, PCNA-immunoreactive cells were sparingly detected in the osteonal cavity of the primary osteon and in the periosteum (Fig. 5C).

Double-labeling immunohistochemistry for PCNA and Runx2 revealed that most of the PCNA-immunoreactive cells showed Runx2-immunoreactivity in the osteonal cavity of the incomplete and complete primary osteons at 2 weeks old (Fig. 5D–F).

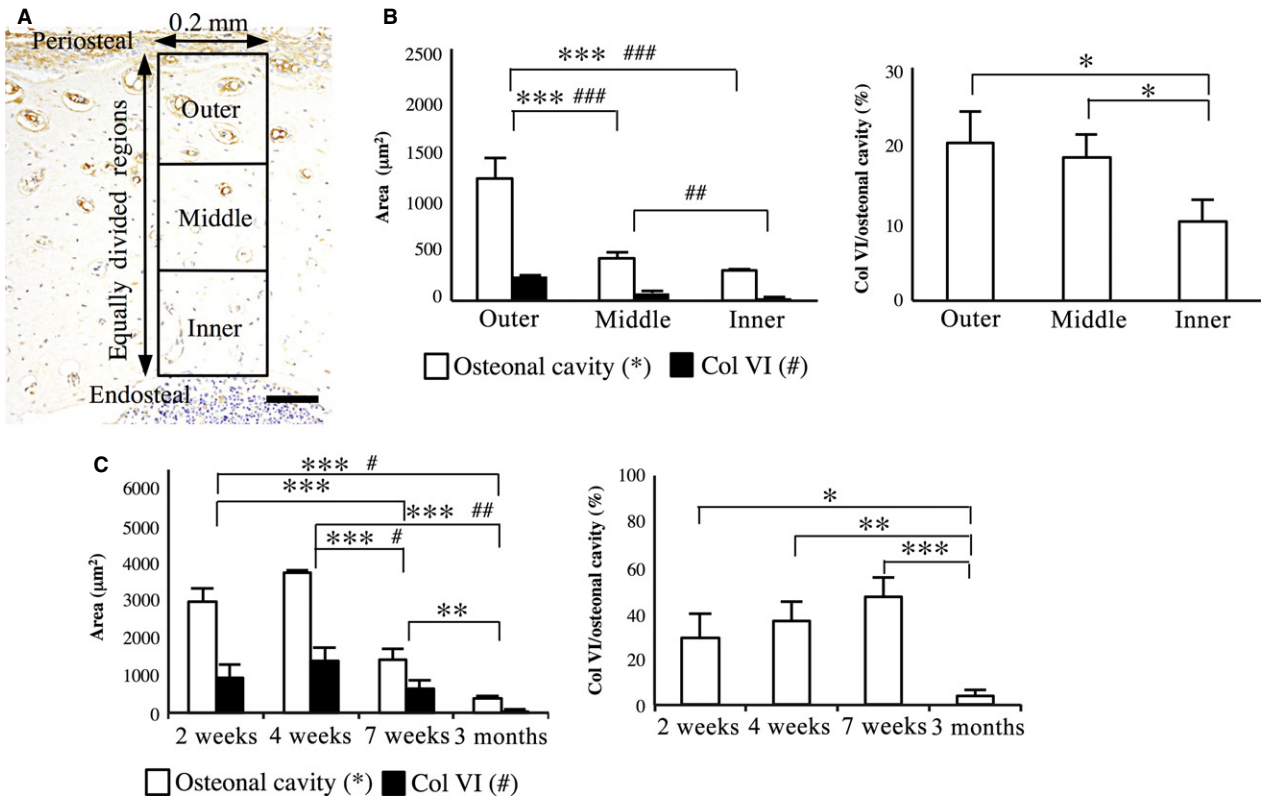

Fig. 3 Analysis of the osteonal cavity area and Col VI-immunoreactive area. (A) Col VI-immunohistochemistry, illustrating the equally divided three regions of the cortical bone for the analysis. Scale bar: 100 μm. (B) The osteonal cavity area, Col VI-immunoreactive area (left panel) and the percentage of Col VI-immunoreactive area to the osteonal cavity area (right panel) in outer, middle, and inner region at 7 weeks. (C) The osteonal cavity area, Col VI-immunoreactive area and the percentage of the Col VI-immunoreactive area to the osteonal cavity area in the upper cortical regions at 2, 4, 7 weeks and 3 months. Data represent mean ± SD. Significant differences were analyzed by one-way ANOVA and Tukey *post hoc* test (*,#$P < 0.05$; **,##$P < 0.01$; ***,###$P < 0.001$).

NG2-immunohistochemistry

At 1 day and 1 week old, NG2-immunoreactivity was localized in the ECM and the cytoplasm of spindle cells in the vascular cavities of the cortical bone. In addition, immunoreactivity was also detected in osteoblasts lining the surface of bone trabeculae. However, spindle cells in the periosteum did not show immunoreactivity (data not shown).

From 2 to 7 weeks old, NG2-immunoreactivity was detected in the spindle cells in the perivascular area and in the osteoblasts lining the perivascular bone surface in the incomplete and complete primary osteons (Fig. 6A,B). In the periosteum, immunoreactivity was detected in a small number of spindle cells and osteoblasts on the surface of the cortical bone.

At 2 and 3 months old, NG2-immunoreactivity was detected in the pericytes and spindle-shaped cells surrounding the blood vessels in the complete primary osteons (Fig. 6C). Immunoreactivity was not detected in the periosteum.

Double-immunofluorescence staining for NG2 and Runx2 and for NG2 and Col VI revealed that most of the Runx2-immunoreactive spindle cells and osteoblasts showed NG2-immunoreactivity and were localized in the Col VI-immunoreactive ECM in the osteonal cavity of the incomplete and complete primary osteons at 2 weeks old (Fig. 6D–I).

Discussion

During osteonal bone formation, periosteal bone growth progresses by an increase in primary osteons at the periphery of the cortical bone, followed by apposition of bone tissue on the perivascular bone surface to fill the primary osteon (Enlow, 1962a,b; Currey, 1984a,b,c; de Margerie et al. 2004). Our histological study indicates that the primary osteon initially appears as the incomplete primary osteon at the periosteal bone surface. Two ridges of bone trabeculae of the incomplete primary osteon were thought to extend and completely enclose the osteonal cavity to form the complete primary osteon.

In the present study, we detected intense localization of Col VI in the ECM in the osteonal cavity of the incomplete and complete primary osteons in young growing rats. Col VI -immunoreactivity was faint in the ECM of the periosteum in all the rats evaluated, and in the expanded vascular cavities in the cortical bone of the neonatal rats aged 1 day

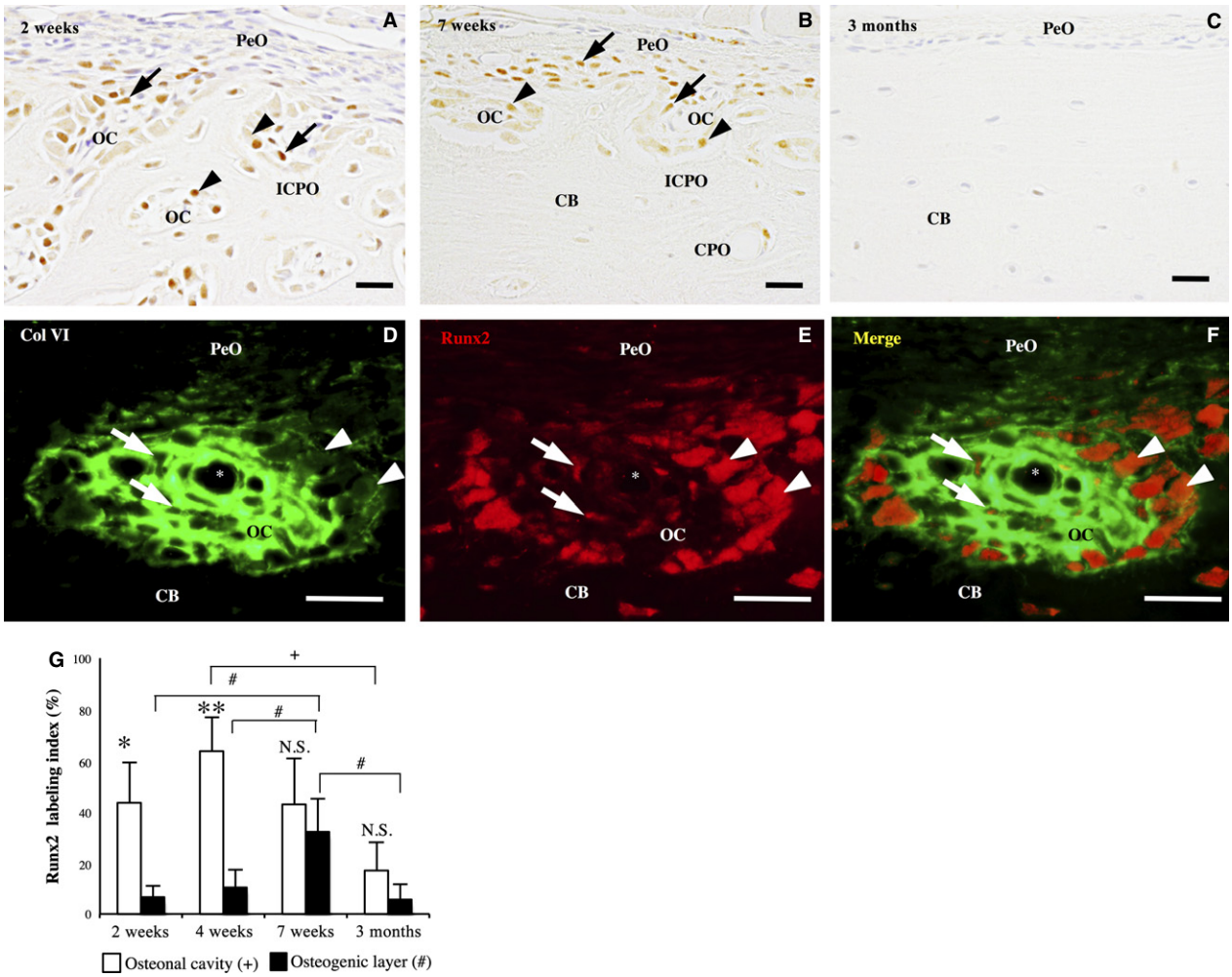

Fig. 4 Runx2-immunohistochemistry of the femoral diaphysis. (A) and (B) At 2 (A) and 7 (B) weeks old, the immunoreactivity is detected in the cuboidal osteoblasts (arrowheads) and spindle cells (arrows) in the osteonal cavity (OC) of the incomplete (ICPO) and complete primary osteons (CPO). (C) At 3 months old, no immunoreactive cells are detected. (D–F) Double-labeling immunohistochemistry for Col VI (green) and Runx2 (red) shows Runx2-immunoreactive spindle cells (arrow) and cuboidal osteoblasts (arrowhead) in the Col VI-immunoreactive ECM in the primary osteon. CB, cortical bone; asterisk, blood vessel. Scale bars: 20 μm. (G) Runx2 labeling index in the osteonal cavity and osteogenic layer at 2, 4, 7 weeks and 3 months. Data represent mean ± SD. Significant differences were analyzed by Student's *t*-test (osteonal cavity vs. osteogenic layer; N.S. not significant, $*P < 0.05$, $**P < 0.01$) or one-way ANOVA and Tukey *post hoc* test (between the 2, 4, 7 weeks and 3 months; +,#$P < 0.05$).

and 1 week. These findings indicate that Col VI provides a characteristic microenvironment in the osteonal cavity of the primary osteon. Col VI deposition initially appeared in the osteonal cavity of the incomplete primary osteon, which was still connected to the periosteum without separation by the bone trabeculae. The immunoreactivity was reduced or disappeared in the osteonal cavities as the primary osteons became smaller toward the endosteum of the cortical bone. Furthermore, in 2- and 3-month-old rats showing no incomplete primary osteons, Col VI-immunoreactivity disappeared in the primary osteons with small osteonal cavities. These results suggest that Col VI in the ECM of the osteonal cavity plays important roles in the formation and development of the primary osteon and decreases as the primary osteon becomes mature.

In the primary osteons of outer cortical regions, Runx2-immunoreactivity was detected in the small spindle cells distributed in the perivascular area and in cuboidal osteoblasts lining the bone surface in young growing rats aged 2–7 weeks. Runx2 is a key transcription factor essential for osteoblast differentiation (Ducy et al. 1997), and is strongly expressed in pre-osteoblasts, immature osteoblasts and early mature osteoblasts during the membranous ossification (Maruyama et al. 2007). Several studies revealed that spindle-shaped cells showing Runx2 expression were pre-osteoblasts or immature osteoblast in the periosteum and bone marrow cavities (Amir et al. 2007; Maruyama et al. 2007; Clarke, 2008; Kodama et al. 2009). Thus, our results indicate that differentiation of osteoblast-lineage spindle cells into mature osteoblasts occurs in the osteonal cavities

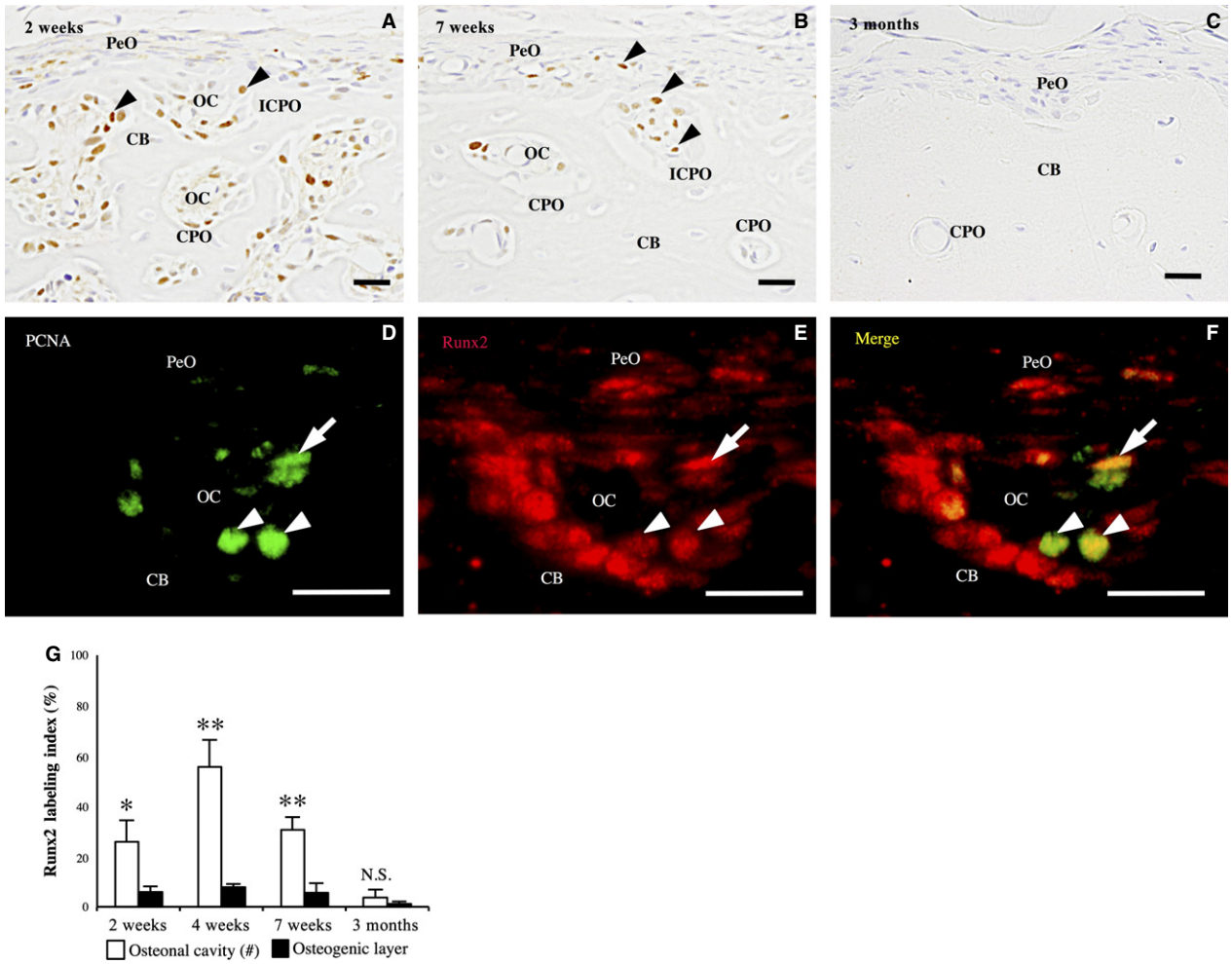

Fig. 5 PCNA-immunohistochemistry of the femoral diaphysis. (A) At 2 weeks old, many immunoreactive cells (arrowheads) are detected in the osteonal cavity (OC) of incomplete (ICPO) and complete primary osteons (CPO); however, only a few are detected in the periosteum (PeO). (B) At 7 weeks old, the immunoreactive cells (arrowheads) are detected mainly in the ICPO and CPO in the outermost region of the cortical bone (CB). (C) At 3 months old, no immunoreactive cells are detected. (D–F) Double-labeling immunohistochemistry for PCNA (green) and Runx2 (red) shows PCNA-immunoreactive spindle cells (arrow) and cuboidal osteoblasts (arrowhead) express Runx2. CB, cortical bone. Scale bars: 20 μm. (G) The panel shows the PCNA labeling index in the osteonal cavity and osteogenic layer at 2, 4, 7 weeks and 3 months old. Data represent mean ± SD. Significant differences were analyzed by Student's *t*-test (osteonal cavity vs. osteogenic layer; N.S. not significant, $*P < 0.05$, $**P < 0.01$).

of the primary osteons. In addition, double-labeling immunohistochemistry for Runx2 and PCNA revealed that some of the osteoblast lineages in the primary osteon showed proliferation activity from 2 to 7 weeks. The numbers of PCNA-immunoreactive cells were significantly higher in the primary osteons than in the osteogenic layer of the periosteum. Taken together with the result that Runx2-immunoreactive cells were more abundant in the primary osteon than in the periosteum, these results indicate that proliferation and differentiation of osteoblast lineages occur mainly in the primary osteon rather than in the periosteum during the growing periods in rats.

Our double-labeling immunohistochemistry confirmed that Runx2-immunoreactive osteoblast lineages were more abundant in Col VI-immunoreactive areas in the primary osteon than in the periosteum showing no Col VI accumulation. At 7 weeks old, Runx2- and PCNA-immunoreactive cells decreased in conjunction with the reduction of the Col VI-immunoreactive areas in the primary osteons. In human osteoblast lineages, Col VI promotes type I collagen expression in the early phase of differentiation, resulting in acceleration of bone matrix mineralization (Ishibashi et al. 1999; Harumiya et al. 2002). Col VI deficiency leads to a disorganized border between the osteoblasts and the bone matrix at the periosteal surface of the cortical bone (Izu et al. 2012). Furthermore, Col VI is known to stimulate proliferation of various mesenchymal cell types (Atkinson et al. 1996; Rühl et al. 1999a). It is therefore possible that Col VI regulates differentiation and proliferation of osteoblast lineages in the incomplete and complete primary osteons.

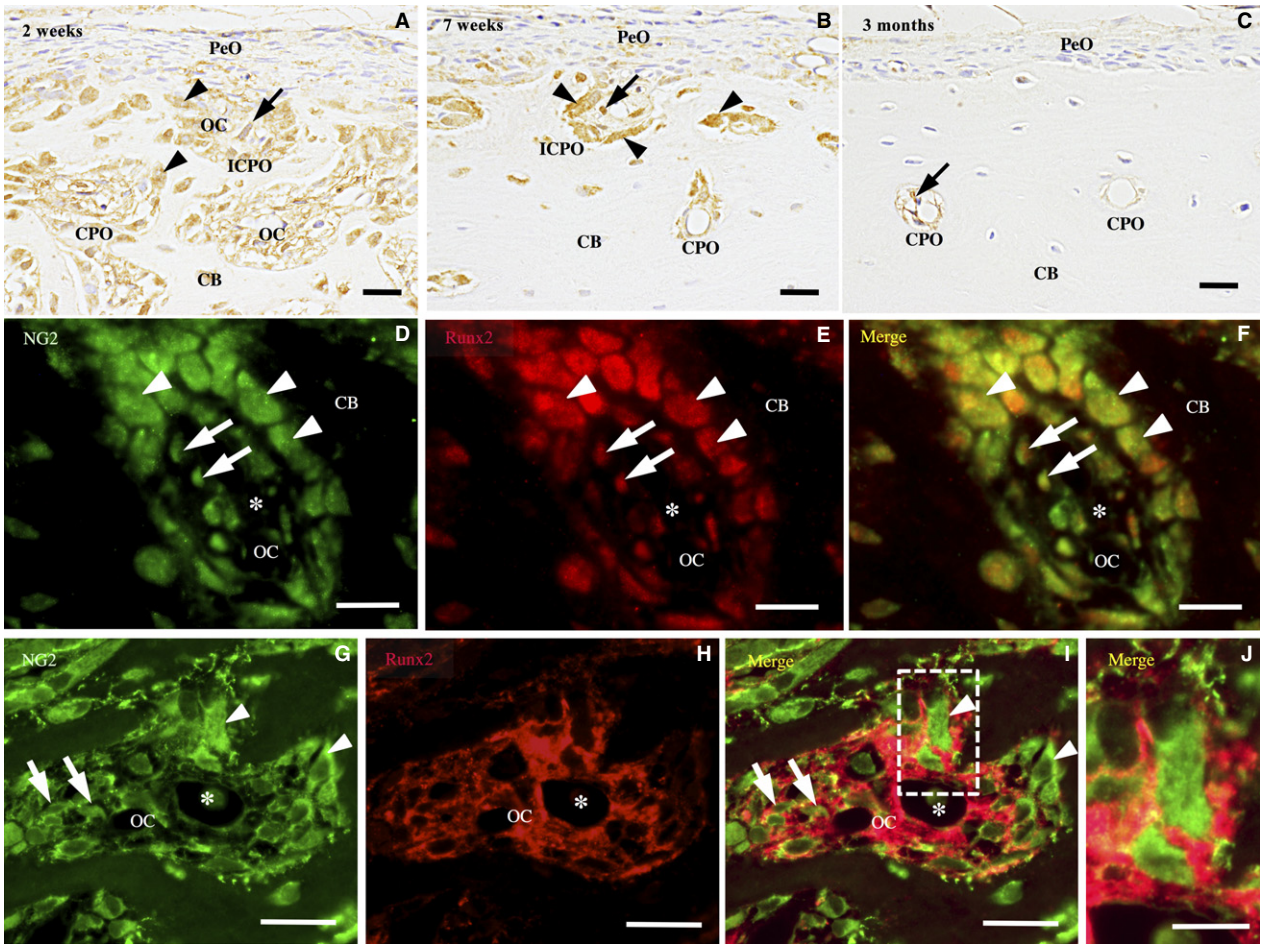

Fig. 6 NG2-immunohistochemistry of the femoral diaphysis. (A) At 2 weeks, NG2 immunoreactivity is found in the cuboidal osteoblasts (arrowheads) and spindle cells (arrows) in the osteonal cavity (OC) of the incomplete (ICPO) and complete primary osteons (CPO). (B) At 7 weeks, the immunoreactive spindle cells (arrows) and osteoblasts (arrowheads) are detected mainly in the ICPOs. (C) At 3 months, a few or no NG2-immunoreactive spindle cells (arrows) are detected in the CPO. (D–F) Double-labeling immunohistochemistry for NG2 (green) and Runx2 (red) shows NG2-immunoreactive spindle cells (arrow) and cuboidal osteoblasts (arrowhead) express Runx2. (G–I) Double-labeling immunohistochemistry for NG2 (green) and Col VI (red) shows NG2-immunoreactive spindle cells (arrow) and cuboidal osteoblasts (arrowhead) in the Col VI-immunoreactive ECM. (J) A high-magnification view of the boxed area. Asterisk, blood vessel. (A–I) Scale bars: 20 μm. (J) Scale bar: 10 μm.

In non-osteogenic cells, Col VI interacts with NG2 on cytoplasmic membranes to promote cell proliferation, spreading and motility by triggering intracellular signaling downstream of NG2 (Burg et al. 1996, 1998; Tillet et al. 2002). Fukushi et al. (2003) demonstrated that NG2 was expressed in osteoblasts delineating newly formed trabecular bones, and was upregulated during the membranous and endochondral ossification in the developing mouse. Thus, NG2 is thought to be one of the essential factors for bone formation by osteoblasts. Our results revealed that Runx2-immunoreactive spindle cells and osteoblasts showed NG2-immunoreactivity in the Col VI-immunoreactive areas in the primary osteon. These results indicate that NG2 is expressed in osteoblast lineages at a wide range of differentiation stages, and functions as a cell-surface receptor that mediates differentiation and proliferation of these cells in response to Col VI in the primary osteon.

NG2 regulates cell–ECM interactions also by collaborating with α3β1 and α4β1 integrins (Iida et al. 1995; Fukushi et al. 2004). In a melanoma cell line, concomitant stimulation of NG2 and α4β1 integrin enhances FAK and ERK1/2 activation (Yang et al. 2004). Col VI binds to α1β1, α2β1 and α3β1 integrins, as well as NG2, implying that NG2 interacts with Col VI in synergy with integrins (Doane et al. 1998; Midwood & Salter, 2001). In osteoblasts, Runx2 activation is mediated by the FAK/ERK pathway, leading to induction of osteoblastic differentiation (Xiao et al. 2000; Schneider et al. 2011). Taken together, it is possible that the Col VI-NG2/integrin interaction will activate Runx2 and upregulate osteoblast lineage differentiation via the FAK/ERK signaling pathway in the primary osteon.

In the incomplete and complete primary osteons, most of Runx2-immunoreactive spindle cells were distributed in the perivascular area, whereas Runx2-immunoreactive

cuboidal osteoblasts localized near or on the bone surface in the osteonal cavity. Thus, it is implied that the differentiation of osteoblast lineages progressed radially from the perivascular area toward the peripheral areas of the osteonal cavity. Consequently, mature osteoblasts may be arranged peripherally and form the bone tissue around the osteonal cavity, leading to the construction of the primary osteon. Interaction of Col VI and NG2 may be concerned with such a formation pattern of the primary osteon by regulating the differentiation and proliferation of osteoblast lineages.

In conclusion, we demonstrated that Col VI was highly accumulated in the osteonal cavity of the primary osteon in the femoral diaphysis of growing young rats. In these regions, spindle cells in the perivascular area and mature osteoblasts lining on the bone surface expressed Runx2. Furthermore, some of the Runx2-immunoreactive spindle cells showed PCNA-immunoreactivity. These findings indicate that osteoblast-lineage spindle cells proliferate and differentiate into mature osteoblasts in the Col VI-rich area in the primary osteon. The Runx2-immunoreactive osteoblast lineages expressed NG2, suggesting that NG2–Col VI interaction may regulate osteoblast lineages and the formation of the primary osteon.

Author contributions

Concept/design: Y. Kohara, S. Soeta. Acquisition of data: Y. Kohara, S. Soeta. Data analysis/interpretation: Y. Kohara, S. Soeta. Drafting the manuscript: Y. Kohara, S. Soeta, Y. Izu. Critical revision: all authors. Approval of the article: all authors.

References

Alroy J, Goyal V, Skutelsky E (1987) Lectin histochemistry of mammalian endothelium. *Histochemistry* **86**, 603–607.

Amir LR, Li G, Schoenmaker T, et al. (2007) Effect of thrombin peptide 508 (TP508) on bone healing during distraction osteogenesis in rabbit tibia. *Cell Tissue Res* **330**, 35–44.

Atkinson JC, Rühl M, Becker J, et al. (1996) Collagen VI regulates normal and transformed mesenchymal cell proliferation *in vitro*. *Exp Cell Res* **228**, 283–291.

Bashey RI, Philips N, Insinga F, et al. (1993) Increased collagen synthesis and increased content of type VI collagen in myocardium of tight skin mice. *Cardiovasc Res* **27**, 1061–1065.

Burg MA, Tillet E, Timpl R, et al. (1996) Binding of the NG2 proteoglycan to type VI collagen and other extracellular matrix molecules. *J Biol Chem* **271**, 26 110–26 116.

Burg MA, Grako KA, Stallcup WB (1998) Expression of the NG2 proteoglycan enhances the growth and metastatic properties of melanoma cells. *J Cell Physiol* **177**, 299–312.

Carter DH, Sloan P, Aaron JE (1991) Immunolocalization of collagen types I and III, tenascin, and fibronectin in intramembranous bone. *J Histochem Cytochem* **39**, 599–606.

Christensen SE, Coles JM, Zelenski NA, et al. (2012) Altered trabecular bone structure and delayed cartilage degeneration in the knees of collagen VI null mice. *PLoS ONE* **7**, e33397. doi:10.1371/journal.pone.0033397.

Clarke B (2008) Normal bone anatomy and physiology. *Clin J Am Soc Nephrol* **3**, S131–S139.

Currey JD (1984a) Can strains give adequate information for adaptive bone remodeling? *Calcif Tissue Int* **36**, 118–122.

Currey JD (1984b) Effects of differences in mineralization on the mechanical properties of bone. *Philos Trans R Soc Lond B Biol Sci* **304**, 509–518.

Currey JD (1984c) What should bones be designed to do? *Calcif Tissue Int* **36**, 7–10.

Doane KJ, Yang G, Birk DE (1992) Corneal cell-matrix interactions: type VI collagen promotes adhesion and spreading of corneal fibroblasts. *Exp Cell Res* **200**, 490–499.

Doane KJ, Howell SJ, Birk DE (1998) Identification and functional characterization of two type VI collagen receptors, alpha 3 beta 1 integrin and NG2, during avian corneal stromal development. *Invest Ophthalmol Vis Sci* **39**, 263–275.

Ducy P, Zhang R, Geoffroy V, et al. (1997) Osf2/Cbfa1: a transcriptional activator of osteoblast differentiation. *Cell* **89**, 747–754.

Enlow DH (1962a) Functions of the Haversian system. *Am J Anat* **110**, 269–305.

Enlow DH (1962b) A study of the post-natal growth and remodeling of bone. *Am J Anat* **110**, 79–101.

Enlow DH, Brown SO (1958) A comparative histological study of fossil and recent bone tissues. Part III. *Tex J Sci* **10**, 187–230.

Everts V, Niehof A, Jansen D, et al. (1998) Type VI collagen is associated with microfibrils and oxytalan fibers in the extracellular matrix of periodontium, mesenterium and periosteum. *J Periodontal Res* **33**, 118–125.

Fan W, Crawford R, Xiao Y (2008) Structural and cellular differences between metaphyseal and diaphyseal periosteum in different aged rats. *Bone* **42**, 81–89.

Fitzgerald J, Rich C, Zhou FH, et al. (2008) Three novel collagen VI chains, α4(VI), α5(VI), and α6(VI). *J Biol Chem* **283**, 20 170–20 180.

Fukushi J, Inatani M, Yamaguchi Y, et al. (2003) Expression of NG2 proteoglycan during endochondral and intramembranous ossification. *Dev Dyn* **228**, 143–148.

Fukushi J, Makagiansar IT, Stallcup WB (2004) NG2 proteoglycan promotes endothelial cell motility and angiogenesis via engagement of galectin-3 and alpha3beta1 integrin. *Mol Biol Cell* **15**, 3580–3590.

Gara SK, Grumati P, Urciuolo A, et al. (2008) Three novel collagen VI chains with high homology to the α3 chain. *J Biol Chem* **283**, 10 658–10 670.

Gattazzo F, Urciuolo A, Bonaldo P (2014) Extracellular matrix: a dynamic microenvironment for stem cell niche. *Biochim Biophys Acta* **1840**, 2506–2519.

Ham AW (1987) Bone. In: *Ham's Histology*. (eds David H, Cormack LB), pp. 280–282. Lippincott Company: Philadelphia, PA, USA.

Harumiya S, Gibson MA, Koshihara Y (2002) Antisense suppression of collagen VI synthesis results in reduced expression of collagen I in normal human osteoblast-like cells. *Biosci Biotechnol Biochem* **66**, 2743–2747.

Hu J, Higuchi I, Shiraishi T, et al. (2002) Fibronectin receptor reduction in skin and fibroblasts of patients with Ullrich's disease. *Muscle Nerve* **26**, 696–701.

Iida J, Meijne AM, Spiro RC, et al. (1995) Spreading and focal contact formation of human melanoma cells in response to

the stimulation of both melanoma-associated proteoglycan (NG2) and alpha 4 beta 1 integrin. *Cancer Res* **55**, 2177–2185.

Ishibashi H, Harumiya S, Koshihara Y (1999) Involvement of type VI collagen in interleukin-4-induced mineralization by human osteoblast-like cells *in vitro*. *Biochim Biophys Acta* **1472**, 153–164.

Izu Y, Ansorge HL, Zhang G, et al. (2010) Dysfunctional tendon collagen fibrillogenesis in collagen VI null mice. *Matrix Biol* **30**, 53–61.

Izu Y, Ezura Y, Mizoguchi F, et al. (2012) Type VI collagen deficiency induces osteopenia with distortion of osteoblastic cell morphology. *Tissue Cell* **44**, 1–6.

Kodama N, Nagata M, Tabata Y, et al. (2009) A local bone anabolic effect of rhFGF2-impregnated gelatin hydrogel by promoting cell proliferation and coordinating osteoblastic differentiation. *Bone* **44**, 699–707.

de Margerie E, Robin JP, Verrier D, et al. (2004) Assessing a relationship between bone microstructure and growth rate: a fluorescent labeling study in the king penguin chick (*Aptenodytes patagonicus*). *J Exp Biol* **207**, 869–879.

Maruyama Z, Yoshida CA, Furuichi T, et al. (2007) Runx2 determines bone maturity and turnover rate in postnatal bone development and is involved in bone loss in estrogen deficiency. *Dev Dyn* **236**, 1876–1890.

Mathews S, Bhonde R, Gupta PK, et al. (2012) Extracellular matrix protein mediated regulation of the osteoblast differentiation of bone marrow derived human mesenchymal stem cells. *Differentiation* **84**, 185–192.

Midwood KS, Salter DM (2001) NG2/HMPG modulation of human articular chondrocyte adhesion to type VI collagen is lost in osteoarthritis. *J Pathol* **195**, 631–635.

Mulliken JB, Glowacki J (1980) Induced osteogenesis for repair and construction in the craniofacial region. *Plast Reconstr Surg* **65**, 553–559.

Nilsson SK, Debatis ME, Dooner MS, et al. (1998) Immunofluorescence characterization of key extracellular matrix proteins in murine bone marrow *in situ*. *J Histochem Cytochem* **46**, 371–377.

Nishiyama A, Stallcup WB (1993) Expression of NG2 proteoglycan causes retention of type VI collagen on the cell surface. *Mol Biol Cell* **4**, 1097–1108.

Pfaff M, Aumailley M, Specks U, et al. (1993) Integrin and Arg-Gly-Asp dependence of cell adhesion to the native and unfolded triple helix of collagen type VI. *Exp Cell Res* **206**, 167–176.

Ramasamy SK, Kusumbe AP, Wang L, et al. (2014) Endothelial Notch activity promotes angiogenesis and osteogenesis in bone. *Nature* **507**, 376–380.

Rühl M, Johannsen M, Atkinson J, et al. (1999a) Soluble collagen VI induces tyrosine phosphorylation of paxillin and focal adhesion kinase and activates the MAP kinase erk2 in fibroblasts. *Exp Cell Res* **250**, 548–557.

Rühl M, Sahin E, Johannsen M, et al. (1999b) Soluble collagen VI drives serum-starved fibroblasts through S phase and prevents apoptosis via down-regulation of Bax. *J Biol Chem* **274**, 34 361–34 368.

Satomi-Kobayashi S, Kinugasa M, Kobayashi R, et al. (2012) Osteoblast-like differentiation of cultured human coronary artery smooth muscle cells by bone morphogenetic protein endothelial cell precursor-derived regulator (BMPER). *J Biol Chem* **287**, 30 336–30 345.

Schneider GB, Zaharias R, Seabold D, et al. (2011) Integrin-associated tyrosine kinase FAK affects Cbfa1 expression. *J Orthop Res* **29**, 1443–1447.

Soeta S, Mori R, Kodaka T, et al. (2000) Histological disorders related to the focal disappearance of the epiphyseal growth plate in rats induced by high dose of vitamin A. *J Vet Med Sci* **62**, 293–299.

Stallcup WB, Dahlin K, Healy P (1990) Interaction of the NG2 chondroitin sulfate proteoglycan with type VI collagen. *J Cell Biol* **111**, 3177–3188.

Stover SM, Pool RR, Martin RB, et al. (1992) Histological features of the dorsal cortex of the third metacarpal bone mid-diaphysis during postnatal growth in thoroughbred horses. *J Anat* **181**, 455–469.

Tillet E, Ruggiero F, Nishiyama A, et al. (1997) The membrane-spanning proteoglycan NG2 binds to collagens V and VI through the central nonglobular domain of its core protein. *J Biol Chem* **272**, 10 769–10 776.

Tillet E, Gential B, Garrone R, et al. (2002) NG2 proteoglycan mediates beta1 integrin-independent cell adhesion and spreading on collagen VI. *J Cell Biochem* **86**, 726–736.

Tonna E (1974) Electron microscopy of aging skeletal cells. *Lab Invest* **31**, 609–632.

Tulla M, Pentikäinen OT, Viitasalo T, et al. (2001) Selective binding of collagen subtypes by integrin α1I, α2I, and α10I domains. *J Biol Chem* **276**, 48 206–48 212.

Wayner EA, Carter WG (1987) Identification of multiple cell adhesion receptors for collagen and fibronectin in human fibrosarcoma cells possessing unique alpha and common beta subunits. *J Cell Biol* **105**, 1873–1884.

Weyand B, von Schroeder HP (2013) Altered VEGF-A and receptor mRNA expression profiles, and identification of VEGF144 in foetal rat calvaria cells, in coculture with microvascular endothelial cells. *Cell Biol Int* **37**, 713–724.

Xiao G, Jiang D, Thomas P, et al. (2000) MAPK pathways activate and phosphorylate the osteoblast-specific transcription factor, Cbfa1. *J Biol Chem* **275**, 4453–4459.

Yang J, Price MA, Neudauer CL, et al. (2004) Melanoma chondroitin sulfate proteoglycan enhances FAK and ERK activation by distinct mechanisms. *J Cell Biol* **165**, 881–891.